

Full paper

# Effective removing of hexavalent chromium from wasted water by triboelectric nanogenerator driven self-powered electrochemical system – Why pulsed DC is better than continuous DC?



Linglin Zhou<sup>a,b,1</sup>, Di Liu<sup>a,b,1</sup>, Shaoxin Li<sup>a,b,1</sup>, Xing Yin<sup>a,b</sup>, Chunlei Zhang<sup>a,b</sup>, Xinyuan Li<sup>a,b</sup>, Chuguo Zhang<sup>a,b</sup>, Wei Zhang<sup>a,b</sup>, Xia Cao<sup>a,b,\*\*</sup>, Jie Wang<sup>a,b,\*\*\*</sup>, Zhong Lin Wang<sup>a,b,c,\*</sup>

<sup>a</sup> Beijing Institute of Nanoenergy and Nanosystems, Chinese Academy of Sciences, Beijing, 100083, China

<sup>b</sup> College of Nanoscience and Technology, University of Chinese Academy of Sciences, Beijing 100049, PR China

<sup>c</sup> School of Materials Science and Engineering, Georgia Institute of Technology, Atlanta, GA, 30332, USA

## ARTICLE INFO

## ABSTRACT

## Keywords:

Triboelectric nanogenerators  
Self-powered system  
Heavy metal treatment  
Pulsed direct current  
Maximize removal efficiency

Electrochemical techniques have been extensively applied to treat heavy metal pollution in our daily life. Traditional electrochemistry is always driven by continuous DC (CDC), but the energy harvested in environment from water using nanogenerator is always a pulsed DC (PDC). The question is if the CDC has a better performance than PDC? Here, we systematically investigated the electrochemical performance of hexavalent chromium (Cr(VI)) removal from waste as powered by pulsed output of triboelectric nanogenerator (TENG) using the energy harvested from environment. By optimizing the frequency and on-off ratio of PDC, the removal efficiency of Cr(VI) can be maximally enhanced by 53.5% compared to that driven by a CDC under equal amount of electric charges, which is further confirmed by electrochemical experiments driven by layered TENG. The reason is the more production of  $\text{Fe}^{2+}$ , the better utilization of  $\text{Fe}^{2+}$ , and the higher ion diffusion rate during the process driven by PDC, where the electrode passivation caused by concentration polarization of the anode region and over potential is reduced. Besides, a self-powered system is designed for removing contaminant from wastewater by harvesting energy from the flowing water through rotary-TENG, where heavy metal pollutant such as Cr(VI) can be sufficiently and continuously removed. This study demonstrate the feasibility and effectiveness of self-powered electrochemical for cleaning environment pollution using the harvested energy.

## 1. Introduction

The growth in water pollution due to the increasing civilization and industrial activities has caused serious environmental problem on a global scale [1]. Toxic heavy metals have been a primary threat to human health and environmental security hazard around the world because they are high toxic, not biodegradable, and tend to accumulate in living tissues throughout the food chain [2]. As one of a typical toxic heavy metal, chromium usually presents in its oxyanion state with high degree of toxicity [3,4]. Peculiarly, hexavalent chromium [Cr(VI)] is extremely toxic and carcinogenic due to its strong oxidizing properties and always causes health problems such as liver damage, pulmonary congestions, vomiting, and severe diarrhea [5], whereas trivalent

chromium [Cr(III)] is a natural form in the earth's crust with a low toxicity even in a high dosage and can be readily precipitated out of solution in the form of  $\text{Cr(OH)}_3$  [6]. Therefore, removal of Cr(VI) or conversion it into Cr(III) prior to discharge into the ecological system is the key to long-term environmental sustainability.

A variety of technologies for heavy metal removal have been demonstrated such as adsorption [7], ion exchange [8], membrane separation [9], which often require excessive co-reagents or sophisticated processes, and can suffer secondary pollution. Over the last decades, as one of the electrochemical technology, electrocoagulation (EC) has been successfully used for removing heavy metals with the features of operation simplicity, rapid kinetics, low operation cost, and environmental compatibility [10,11]. However, electrode passivation induced

\* Corresponding author. Beijing Institute of Nanoenergy and Nanosystems, Chinese Academy of Sciences, Beijing, 100083, China.

\*\* Corresponding author. College of Nanoscience and Technology, University of Chinese Academy of Sciences, Beijing, 100049, PR China.

\*\*\* Corresponding author. College of Nanoscience and Technology, University of Chinese Academy of Sciences, Beijing, 100049, PR China.

E-mail addresses: [caoxia@binn.cas.cn](mailto:caoxia@binn.cas.cn) (X. Cao), [wangjie@binn.cas.cn](mailto:wangjie@binn.cas.cn) (J. Wang), [zhong.wang@mse.gatech.edu](mailto:zhong.wang@mse.gatech.edu) (Z.L. Wang).

<sup>1</sup> These authors contributed equally to this work.

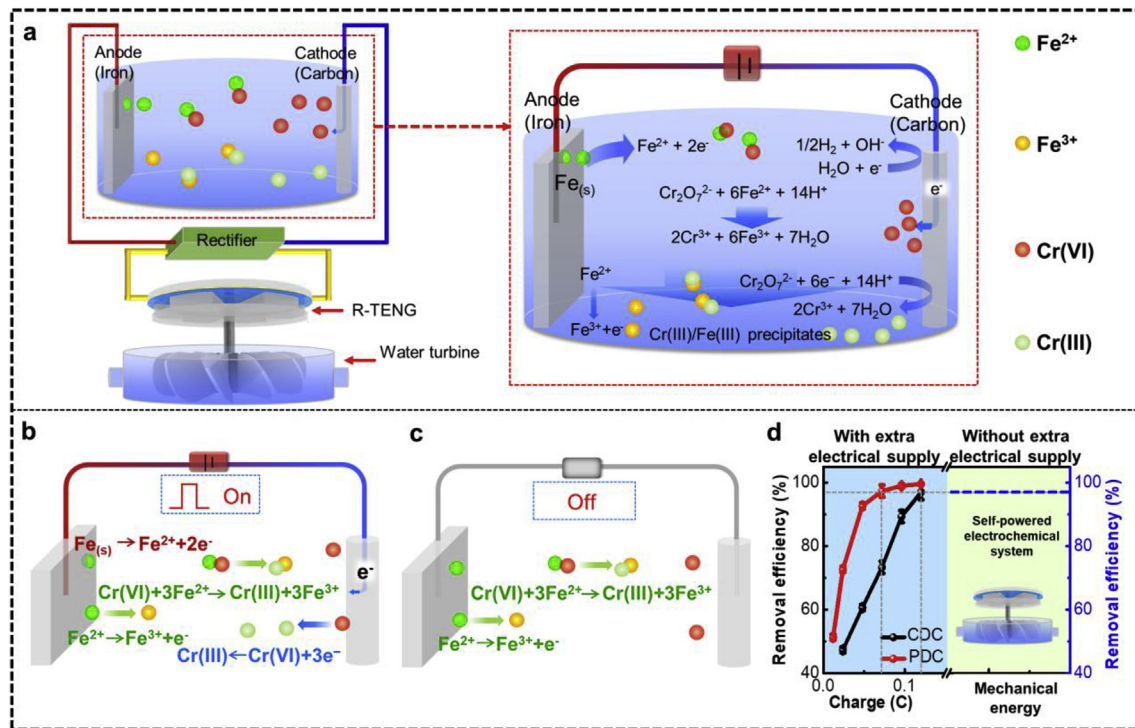


**Fig. 1. The electrochemical reactions of Cr(VI) removal during EC process.** **a** Self-powered system for Cr(VI) removal driven by rectified TENG, insert shows enlarged illustration of the reactions occurring at the surface of the electrode pair during the process of electrochemical. **b** With current in the on state, Cr(VI) is reduced by Fe<sup>2+</sup> and the cathode. **c** With current in the off state, reduction of Cr(VI) to Cr(III) by Fe<sup>2+</sup> in the solution occurs. **d** Extra charge consumption during removal of Cr(VI) under different conditions, where the red and black curve are the relationship of removing efficiency of Cr(VI) and the charge consumption driven by PDC and CDC, respectively, and the right part of the image represents the same high removal efficiency can be obtained by a self-powered system without extra electrical supply.

the decline of removal efficiency and the demand of extra external power supply are the key limiting factors that need to be solved for widespread usage of EC. To reduce or even eliminate the electrode passivation, alternating DC have been used to remove heavy metal pollutants instead of common constant direct current (CDC) and the electrochemical performance can be substantially improved by decreasing the concentration polarization and the over voltage of the electrodes [12,13]. However, a lower removal performance of heavy metal pollutants was obtained in this process. Additionally, a self-powered electrical process based on triboelectric nanogenerator (TENG) has been proposed to directly harvest the ambient environment energy for pollutants removal [14–18]. With the improvement of output performance of TENG [19–23], the self-powered system provides a promising technology for solving the extra electric energy supply during electrochemical wastewater treatment and making it a sustainable process.

To maximize the removal efficiency of Cr(VI) and solve the extra power supply during electrochemical treatment, a self-powered system with a PDC output is used to remove Cr(VI) by harvesting energy from the flowing water through rotary-TENG (R-TENG). We firstly investigate the electrochemical removal performance of Cr(VI) driven by PDC compared with CDC. Through optimizing the frequency and on-off ratio, only 0.072C of charge is required to completely remove Cr(VI) (initial concentration of 1 mg L<sup>-1</sup>) driven by PDC, whereas 0.12C of charge is needed driven by CDC, indicating a substantial improvement of electrochemical performance through using PDC. With a specific pulsed signal for TENG, a PDC output based alternate layered TENG (AL-TENG) is fabricated though designing pulsed current waveforms for Cr(VI) removing, and the results also exhibit that electrochemical reaction powered by TENG exhibits a higher removal efficiency than that of CDC. Besides, a self-powered system is fabricated to remove Cr(VI) from wastewater by harvesting energy from the flowing water through

R-TENG. The presented work not only establishes an optimization methodology for electrochemical removal of pollutants from wastewater, but also confirmed the promising application of the self-powered system based on TENG for the simultaneous energy saving and environmental governance.

## 2. Results and discussion

### 2.1. The electrochemical reactions of Cr(VI) removal during EC

Because it only requires minimum chemical reagents during the reaction processes compared with other electrochemical technologies [24,25], EC has become a promising technology for removing toxic heavy metals from wastewater. During a typical reaction processes of EC, metallic ions in-situ generate by electrochemical dissolution/corrosion from sacrificial anode materials as activated intermediates [26,27], whereas the production of hydrogen bubbles typically occurs at cathode. In the case of removing Cr(VI) using EC system, when a potential difference is applied to the electrodes, the following electrochemical reactions can occur [28]:

In the anode, if iron is applied as material, the electrochemical oxidation generates Fe<sup>2+</sup> ions:



Once the over voltage produced on anode, secondary reactions may take place at the Fe surface, which will induce electrode passivation:



In the cathode, water and Cr(VI), in the form of dichromate, are simultaneously reduced according to following reactions:

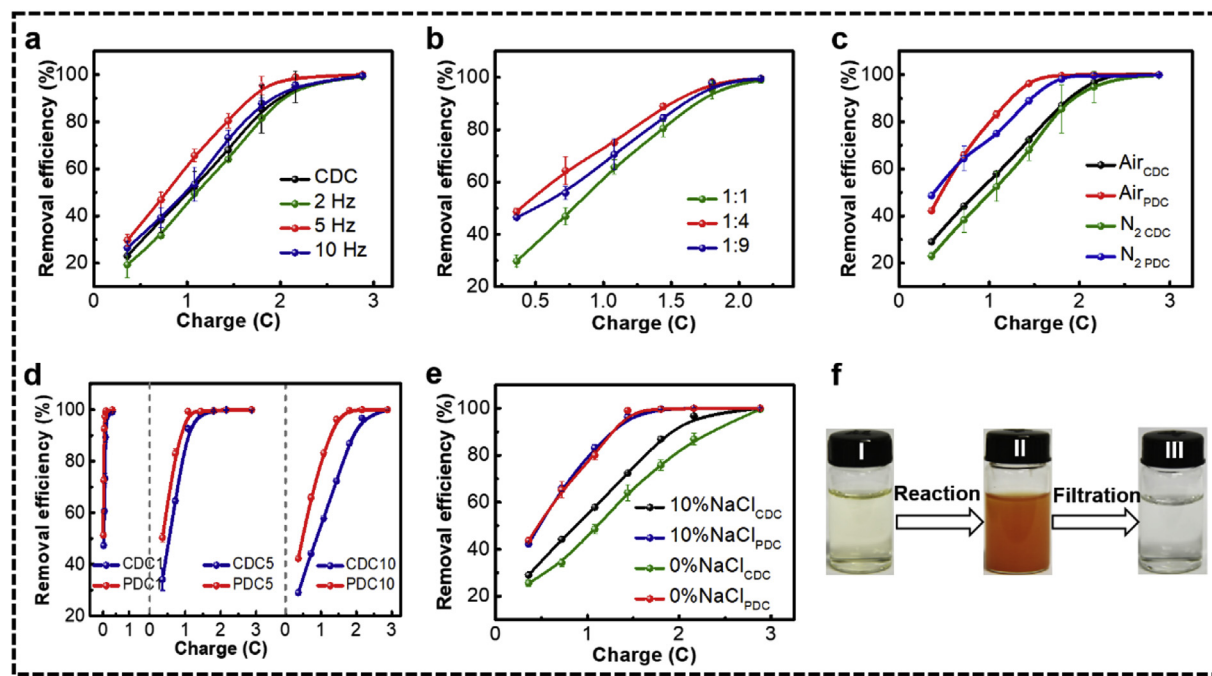
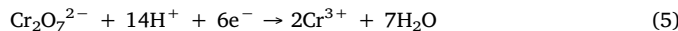
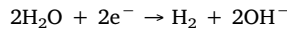
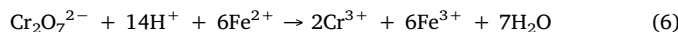


**Fig. 2.** The performance of Cr(VI) removal with CDC and PDC supply at a current of 200  $\mu$ A. **a** The performance of Cr(VI) removal with CDC or PDC at different frequency (2 Hz, 5 Hz, and 10 Hz), respectively (initial concentration Cr(VI) is 10 mg L<sup>-1</sup>). **b** The performance of Cr(VI) removal with PDC in 5 Hz with different on-off ratio, respectively (initial concentration Cr(VI) is 10 mg L<sup>-1</sup>). **c-e** The effect of initial concentration of Cr(VI) (1 mg L<sup>-1</sup>, 5 mg L<sup>-1</sup>, and 10 mg L<sup>-1</sup>), gas atmospheres, and concentration of NaCl on Cr(VI) removal, respectively. **f** The color change of the solution before and after removing Cr(VI) with initial concentration of 10 mg L<sup>-1</sup>.



Besides these electrochemical reactions mentioned above,  $\text{Fe}^{2+}$  ions produced in the Fe surface, can directly reduce Cr(VI) to Cr(III) as the following reaction:



Depending on the solution pH, the produced  $\text{Fe}^{3+}$  spontaneously form various metal hydroxides complexes [29]. As a gelatinous suspension, these compounds still exist in the solution, which can remove the Cr(VI) or Cr(III) from wastewater through complexation, electrostatic attraction, followed by coagulation. The schematic illustrations of the mechanism for Cr(VI) removal are displayed in the **insert of Fig. 1a**.

During the EC system for heavy metals removal, external power is required to supply and removal performance will gradually decline induced by electrode passivation. To solve these problems, a self-powered system of electrochemical unit with PDC output performance is used to remove Cr(VI) by harvesting energy from the flowing water through R-TENG in this work. The system mainly consists of three parts including a R-TENG as power resource, 10% (w/v) NaCl solution as electrolyte, and electrodes (Fig. 1a). Herein, iron plate and graphite rod are selected as anode and cathode respectively, where they are parallel with each other at an inner electrode distance of 2.5 cm. To drive the electrochemical reactions for removing Cr(VI), the above R-TENG connect with a rectifier for transforming the alternating current output into a PDC signal.

The reactions of Cr(VI) removal driven by PDC with the period of turn on ( $T_{on}$ ) and turn off ( $T_{off}$ ) show significant differences. With the period of  $T_{on}$ , Cr(VI) can be reduced through electrons moved from anode to cathode and  $\text{Fe}^{2+}$  ions produced in the Fe surface during the process of electrochemical reaction (Fig. 1b). With the period of  $T_{off}$ , reduction of Cr(VI) to Cr(III) can also occur by  $\text{Fe}^{2+}$  present in the solution (Fig. 1c). In this way, a maximum utilization of  $\text{Fe}^{2+}$  produced in anode can be achieved for removing Cr(VI), thus a higher removal

efficiency of Cr(VI) is obtained using PDC. The detail removal performance and mechanism are described in the following parts.

Generally, the charge is entirely used for pollutant removal without passivation in the Fe-EC process. However, once passivation takes place, a part of the charge will be wasted to produce  $\text{O}_2$  as a consequence of passive film formed on the surface of electrode [30]. Therefore, the charge consumption during Cr(VI) treatment can be used as an index to reflect the removal performance and the extent of passivation. The charge consumption of electrochemical removing Cr(VI) driven by different power is described in Fig. 1d. Through optimizing the frequency (5 Hz) and on-off ratio ( $T_{on}/T_{off} = 1:4$ ), only 0.072C of charge is required to completely remove Cr(VI) (initial concentration of 1 mg L<sup>-1</sup>) driven by PDC, whereas 0.12C of charge is needed driven by CDC. Besides, under equal amount of electric charges (0.048C), the removal efficiencies of Cr(VI) powered by a CDC and PDC are 60% and 92% respectively, demonstrating that the removal efficiency can be maximally enhanced by 53.5% powered by PDC compared to that driven by a CDC. These results indicate that the removal efficiency and electrode passivation are substantially improved through using PDC. With a specific pulsed signal for TENG, a self-powered system based on TENG is fabricated to remove Cr(VI) with high efficiency from wastewater by harvesting energy from the flowing water, where flowing water energy is instead of extra power source to drive electrochemical reaction, greatly lowering the power consumption.

## 2.2. The performance of Cr(VI) removal driven by CDC and PDC

We compared the electrochemical removal performances of Cr(VI) driven by CDC and PDC respectively. Frequency is a key parameter of the PDC as power supply. In order to quantify the influence of conducting frequency on EC performance, experiments are performed with the frequency ranging from 2 to 10 Hz, where a fixed current condition with 200  $\mu$ A was utilized. At the same condition, when total charge consumption is 1.8C, the removal efficiencies of Cr(VI) are 85.3%, 81.6%, 95.4%, and 87.7% with CDC and PDC in 2, 5, 10 Hz supply respectively (Fig. 2a), indicating that the removal efficiency driven by

PDC at 5 Hz is higher than that with CDC supply. This is probably because that it is more difficult for the passive film generating on the electrode surface under PDC supply at 5 Hz, and thus resulting in a decreasing of charge quantity. In addition, a higher frequency at 5 Hz is beneficial to the production of  $\text{Fe}^{2+}$ , and thereby leading to a higher charge efficiency, which will be verified by the next part of experimental results.

On/off ratio is another factor of PDC that affects the electrochemical removal performance. Herein, three on-off time ratios are performed to determine the optimal electrode combinations for Cr(VI) treatment with a range from 1:1 to 1:9, where other PDC parameters are fixed at 200  $\mu\text{A}$ , 5 Hz. As shown in Fig. 2b, the highest removal efficiency (98.2%) is obtained at  $T_{\text{on}}/T_{\text{off}}$  of 1:4 with the equal charge consumption of 1.8C. The increasing of turn-off time at 5 Hz could lead to better utilization of  $\text{Fe}^{2+}$  produced in the anode surface, and thereby decrease the concentration polarization of the Fe electrode surface. At the same time, the intermittent reaction can rises the ion diffuse rate, and the decline of over potential can reduces the electrode passivation [31]. However, continue prolonged  $T_{\text{off}}$  time would lead to ineffective mass transfer during the electrochemical reaction process, resulting a lower removal efficiency of Cr(VI) with  $T_{\text{on}}/T_{\text{off}}$  of 1:9. Therefore, an appropriate parameter of frequency and on/off ratio based on the results is identified as 5 Hz and 1:4, and the following tests were performed under this condition.

A systematic investigation of factors including the atmosphere, initial concentration of Cr(VI), and concentration of electrolytes were carried out to comprehensively estimate the performances of Cr(VI) removal based on CDC and PDC. As shown in Fig. 2c, the removal efficiencies of Cr(VI) with PDC supply are higher compared with those of CDC supply, which is consistent with the previous results. Besides, for the reaction in atmosphere condition, both of removal efficiency based on CDC and PDC exhibits a slightly higher than those reaction in the  $\text{N}_2$  condition, which is because that a small amount of Cr(VI) is reduced by  $\text{Fe}^{2+}$  ions produced in the Fe surface who is exposed to the air (Fig. S1). Additionally, the higher removal efficiency with PDC supply than CDC supply, occurs in different initial concentration of Cr(VI), and the increase rate enhances with the initial concentration increasing from 1  $\text{mg L}^{-1}$  to 10  $\text{mg L}^{-1}$  (Fig. 2d). As shown Fig. 2e, the existence of  $\text{Cl}^-$  can enhance the removal efficiency of Cr(VI) based on both of the PDC and CC supply, which is because the addition of  $\text{Cl}^-$  can increase the conductivity of the solution and slows down the anode passivation, as  $\text{Cl}^-$  ions catalyze the dissolution of the electrode by pitting corrosion<sup>23</sup>. As shown in Fig. 2f from I to III, some flocculated particles generate during the electrochemical reaction, which is beneficial to Cr(VI) removal by attaching pollutants to flocculated particles, thereby the pollutants can be conveniently concentrated, collected, and finally removed.

### 2.3. Process analysis of Cr(VI) removed by CDC or PDC

To compare the process of Cr(VI) removal with CDC and PDC supply, the conductivity and pH change after Cr(VI) removal driven by different power sources are investigated. As shown in Fig. 3a, the initial conductivity of solution is 71.02  $\mu\text{S cm}^{-1}$ . After reaction driven by CDC and PDC, the conductivities increase to 136.25  $\mu\text{S cm}^{-1}$  and 473.5  $\mu\text{S cm}^{-1}$ , respectively. The increase of conductivity after reaction attributes to the  $\text{Fe}^{2+}$  generated in the anode surface during the electrochemical process. Besides, the higher conductivity of the system with PDC supply than that of CDC supply demonstrates that more  $\text{Fe}^{2+}$  produces in the system driven by PDC, indicating that PDC can facilitate the production of  $\text{Fe}^{2+}$ , and thereby resulting in a higher charge efficiency. Besides, an increase of pH change is also observed. With progress driven by CDC and PDC, the solution pH increases from initial value of 6.0 to final values of 6.8 and 7.3 respectively, which is mainly because of the consumption of  $\text{H}^+$ , even though polymeric metal hydroxides increases during EC process [32]. Besides, as flocculated particles, the co-

precipitation of Cr(III) and Fe(III) takes place in this pH range, which is beneficial to the concentration and collection of the pollutants [33].

In addition, the total concentrations of Cr and Fe ions after removing Cr(VI) with CDC or PDC supply are investigated. As shown in Fig. 3b, after removing, the total Cr ions in the system with PDC supply is 0.0073  $\text{mg L}^{-1}$ , which is far lower than that of CDC supply (0.184  $\text{mg L}^{-1}$ ), indicating the more exhaustive reaction in the process driven by PDC. In addition, the total Fe ions in the system with PDC supply (0.046  $\text{mg L}^{-1}$ ) is far higher than that of CDC supply (0.0057  $\text{mg L}^{-1}$ ), further demonstrating the more Fe produces in the former system, which accords well with the previous results.

The formed precipitation in the reaction process were analyzed using XPS. As shown in Fig. 3c, a significant peak at 576 eV attributing to Cr(III) is observed in the Cr2p spectrum [34], demonstrating the reduction of Cr(VI) to Cr(III) in the electrochemical reactions. In addition, the mainly peak at 711 eV in Fe2p spectrum is assigned to the binding energy of 2p3/2 of Fe(III) (Fig. 3d), confirming the reduction of Cr(VI) by  $\text{Fe}^{2+}$  ions [35].

### 2.4. Removing Cr(VI) by a AL-TENG

Based on the above analyses, with the same total charge consumption/transfer, PDC can enhance the removal efficiency of Cr(VI) compared to CDC. Interestingly, the electrical output performance of TENG exhibits a specific pulsed signal, proving a promising method for electrochemical removing heavy metal ions with high efficiency. According to a higher transfer charge density than symmetrical layered structure [36], AL-TENG is fabricated and various PDC waveforms with different frequencies and on/off ratios are designed for Cr(VI) removing. The photograph of the AL-TENG is shown in Fig. S2, and the corresponding working mechanism is shown in Fig. S3 and Note S1. As for Cr(VI) removal driven by AL-TENG (Fig. 4a), the output performances of the AL-TENG are shown in Fig. 4b-f. With the frequency increase, the charge generated by AL-TENG increases fast with an electric quantity of 5.24, 9.82, and 21.4  $\mu\text{C s}^{-1}$  at mechanical triggering frequency of 1, 2, and 5 Hz, respectively (Fig. 4b). The output short-circuit current of the AL-TENG, shown a specific pulsed signals, increases from 97.35  $\mu\text{A}$  to 236.46  $\mu\text{A}$  with the increase of frequency range from 1 Hz to 5 Hz (Fig. 4c), where the maximum current is close to the value (200  $\mu\text{A}$ ) used in the test of CDC and PDC power supply for removing Cr(VI). It can be observed that the open-circuit voltage decreases from 513.52 V to 483.17 V, with the frequency from 1 Hz to 5 Hz (Fig. 4d). These results demonstrate that the charge and short-circuit current increase with the frequency increasing, while the voltage output displays a slight decline. The maximal output power reaches 6.2 mW when connected the matched load of 10  $\text{M}\Omega$  at frequency of 1 Hz (Fig. S4). By the half peak width of turn on time, we can estimate that the  $T_{\text{on}}/T_{\text{off}}$  ratios are 1:4.3, 1:2.5, and 1:2 at frequency of 1, 2, and 5 Hz, respectively (Fig. 4e). All of the values are close to the appropriate parameter of  $T_{\text{on}}/T_{\text{off}}$  ratio as 1:4. The stability of the AL-TENG is also investigated with a frequency of 1 Hz. As shown in Fig. 4f, a total of 6800 cycles of data is recorded and the peak current of per 200 cycles is demonstrated. The inset of Fig. 4f shows the original data for several cycles. After 6800 cycles, the peak current almost keep the same value, indicating the high stability and durability of the AL-TENG, which can be used as power supply to drive electrochemical reaction.

The performance of the AL-TENG for Cr(VI) removal is investigated to compare with that of CDC. As shown in Fig. 4g, under the electric charges such as 0.01897C, the removal efficiencies of Cr(VI) driven by AL-TENG are much higher than that of CDC (below 45%), and the highest removal efficiency is obtained using AL-TENG at the frequency of 5 Hz (98.55%). Besides, the removal performance of Cr(VI) using AL-TENG displays a faster removal rate than that of CDC (Fig. 4h). The above analyses indicate that TENG with a typical pulsed signal can improve the removal efficiency of Cr(VI), thereby provide a promising method to improve the performance of electrochemical removal of

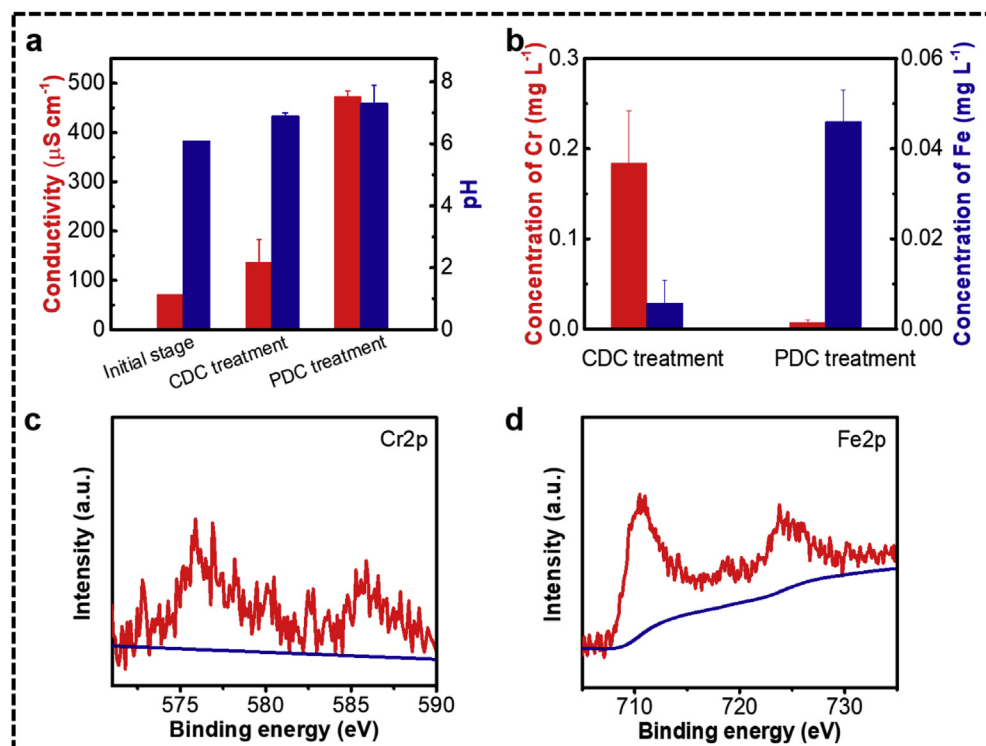


**Fig. 3. Process analysis of Cr(VI) removal by electrochemistry method.** **a** The conductivity and pH change after Cr(VI) removal with CDC or PDC supply (The initial solution only includes  $10 \text{ mg L}^{-1}$  of Cr(VI)). **b** The total concentration of Cr and Fe after removing Cr(VI) with CDC or PDC supply. **c-d** XPS spectra (Cr2p and Fe2p) of precipitate.

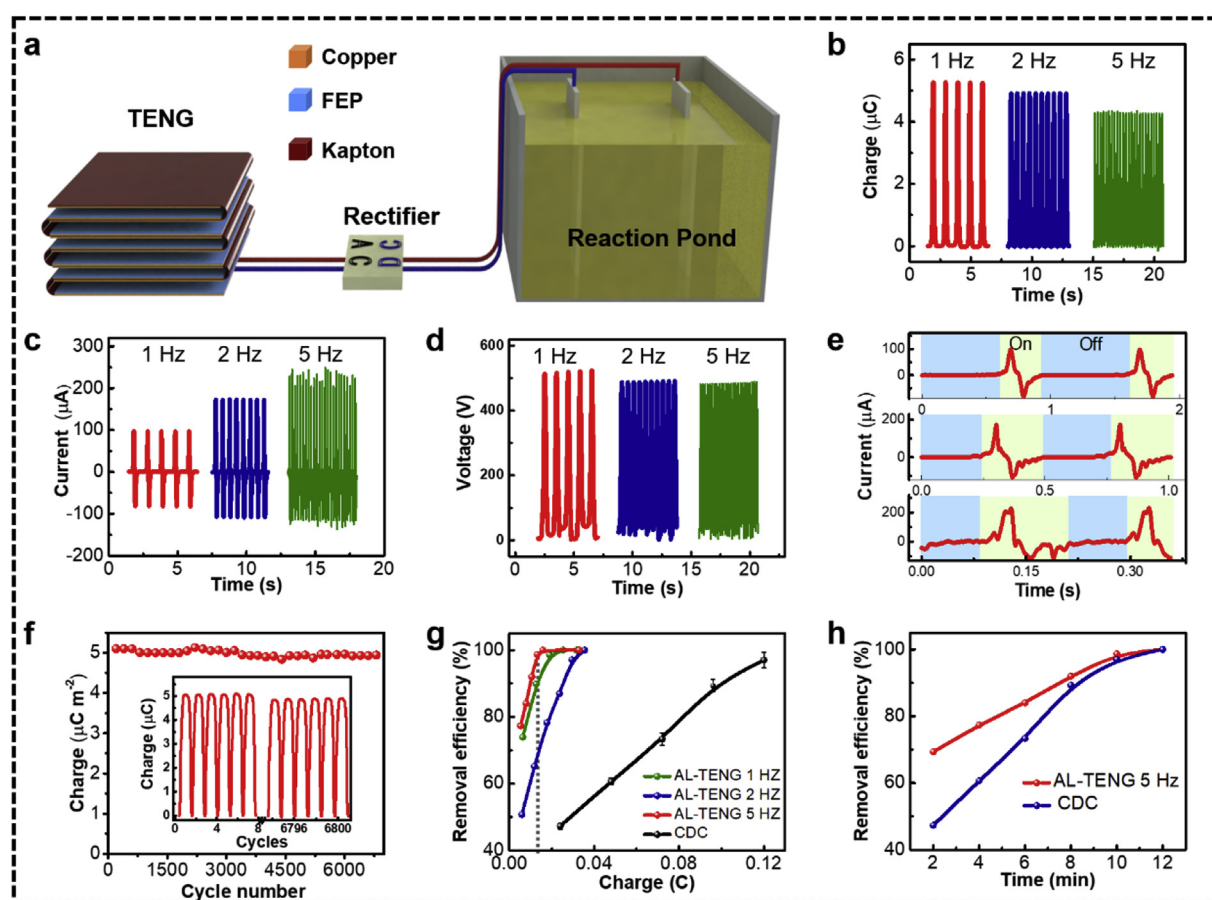


**Fig. 4. Output performance of AL-TENG and its application in removing Cr(VI).** **a** Schematic diagram of removing Cr(VI) driven by AL-TENG. **b-d** Charges, short-circuit current, and open-circuit voltage of AL-TENG under different frequency. **e** The  $T_{\text{on}}/T_{\text{off}}$  ratios of pulsed current based on AL-TENG at different frequency. **f** The long-term output current of the AL-TENG under different cycles. **g** The performance of Cr(VI) removal using constant current driven by electrochemical workstation, and pulse current of AL-TENG at different frequency. **h** The removal performance of Cr(VI) with time increasing using constant current and AL-TENG at 5 Hz.

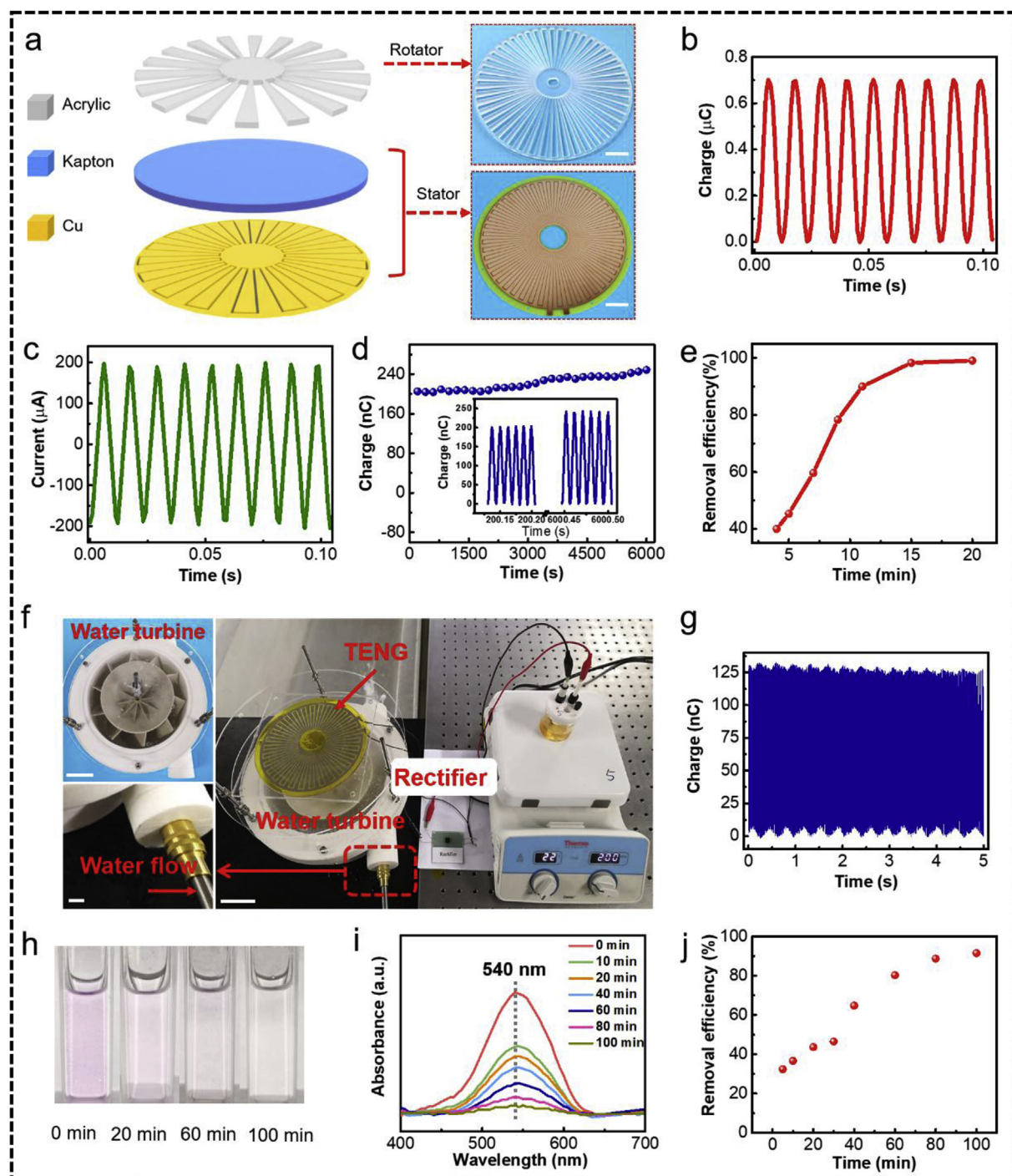


**Fig. 5. Demonstration of the self-powered Cr(VI) treatment system through R-TENG.** **a** Structural design of R-TENG, insert shown the photograph of a stator and a rotator (scale bar, 5 cm). **b** Output charge at a rotation rate of  $100 \text{ r min}^{-1}$ . **c** Short-circuit current at a rotation rate of  $100 \text{ r min}^{-1}$ . **d** The long-term output current of the R-TENG under  $6000 \text{ s}$ . **e** The removal efficiency of Cr(VI) driven by R-TENG. **f** Harvesting energy from water flow at a flow rate of  $6 \text{ L min}^{-1}$  by R-TENG for removing Cr(VI) with initial concentration of  $1 \text{ mg L}^{-1}$  (scale bar, 5cm). Insets: planform of the water turbine (scale bar, 5 cm); tap water is directed into a water turbine through a water gun (scale bar, 1 cm). **g** Output charge of self-powered R-TENG driven by water flow. **h** UV-visible absorption spectra of the Cr(VI) samples with chromogenic reagent for the different working times driven by self-powered system. **i** Corresponding color change of the sample solution for different working times. **j** Corresponding removal efficiency of Cr(VI) for different working times.

pollutants instead of CDC supply.

#### 2.5. Self-powered electrochemical removal of Cr(VI) through a R-TENG

For electrochemical removal of pollutants from wastewater without using an external power source, a self-powered system is fabricated to remove Cr(VI) by harvesting energy from the flowing water through R-

TENG. The R-TENG is mainly composed of a stator and a rotator (Fig. 5a). As for the stator, it consists of a layer of kapton as a triboelectric layer and a layer of electrodes (insert of Fig. 5a). The rotator is fabricated by a disc-shaped acrylic as another triboelectric layer (insert of Fig. 5a). The working mechanism for R-TENG is elaborated in Fig. S5 and Note S2. The output performance is investigated firstly driven by a rotation motor to control the rotation. The generated charge and open-

circuit voltage of R-TENG are  $0.7 \mu\text{C}$  (Figs. 5b) and  $440 \text{ V}$  (Fig. S6a), respectively. At the above rotation rate, the peak output power reaches  $8 \text{ mW}$  when connected to the matched load of  $5 \text{ M}\Omega$  (Fig. S6b). Additionally, the short-circuit current with a continuous alternating pulse signals is  $197.2 \mu\text{A}$  at the rotation rate of  $100 \text{ r min}^{-1}$  (Fig. 5c), and comes to  $583.6 \mu\text{A}$  with the rotating rate increasing to  $300 \text{ r min}^{-1}$  (Fig. S7a). Whereas the transferred charge and open-circuit voltage remain nearly constant value of  $0.7 \mu\text{C}$  and  $440 \text{ V}$  respectively (Figs. S7b and S7c), indicating the large enhancement of short-current with rotating rate increasing. We further investigated the stability of the R-TENG. The charge produced by R-TENG is measured and compared before and after  $6000 \text{ s}$  with continuous operation. As displayed in Fig. 5d, output displayed a minor increase, demonstrating the good durability of the R-TENG. Additionally, the removal efficiency of Cr(VI) driven by R-TENG is surveyed at a rotation rate of  $100 \text{ r min}^{-1}$ . After  $15 \text{ min}$  of treatment, the removal efficiency reaches to  $98.3\%$  (Fig. 5e). With the features of good output performance and operability, R-TENG driven by flowing water is applied to fabricate a self-powered system for electrochemical removing Cr(VI). With water flow rate of  $6 \text{ L min}^{-1}$  (Fig. 5f), the R-TENG can be driven to rotates steady, which can serve as a power source to directly drive electrochemical reaction (Video S1). As shown in Fig. 5g and Figs. S8a–b, the output charge, short circuit current, and open circuit voltage of self-powered system reach about  $130 \text{ nC}$ ,  $25.7 \mu\text{A}$ , and  $224 \text{ V}$ , respectively. As the reaction progress, the UV absorbancy of Cr (VI) declines and the color become light gradually, as shown in Fig. 5h and i. After  $100 \text{ min}$  of removing, the removal efficiency reaches to  $91.5\%$ , indicating that heavy metal pollutant such as Cr(VI) can be sufficiently and continuously removed with only the electrical energy extracted from water flow by the TENG.

Supplementary data related to this article can be found at <https://doi.org/10.1016/j.nanoen.2019.103915>.

### 3. Conclusions

In this work, the electrochemical performance of heavy metal removal driven by PDC or TENG with a specific pulse signal is systematically investigated. The electrochemical performance of Cr(VI) removal driven by PDC with optimized frequency and on-off ratio, can be largely improved than that of CDC. This is because of the more production of  $\text{Fe}^{2+}$ , the better utilization of  $\text{Fe}^{2+}$ , and the higher ion diffusion rate during the process driven by PDC, where the electrode passivation caused by concentration polarization of the anode region and over potential is reduced. With a typical pulse output signal, the removal efficiency of AL-TENG at the frequency of  $5 \text{ Hz}$  ( $98.55\%$ ) is much higher than that of CDC ( $45\%$ ) with the same charge consumption of  $0.01897\text{C}$ , and the reaction driven by AL-TENG also exhibits a faster removal rate than that of CDC at the same reaction time. In this way, TENG with a specific pulse signals provides a promising method to enhance the electrochemical performance for removing heavy metal pollutants. Besides the high removal performance driven by AL-TENG, a self-powered system based a R-TENG is designed to harvest energy from flowing water to electrochemically remove Cr (VI) without supplying an external power. At a flow rate of  $6 \text{ L min}^{-1}$  and initial Cr(VI) concentration of  $1 \text{ mg L}^{-1}$ ,  $91.5\%$  of Cr(VI) can be removed from wastewater in  $100 \text{ min}$  using the generated power, confirmed the promising application of the self-powered system based on TENG for the simultaneous energy saving and environmental governance.

In summary, our study demonstrates an effective approach for enhancing the electrochemical performance of removing heavy ions by using pulsed DC supply instead of the continuous DC due to the more production of  $\text{Fe}^{2+}$ , better utilization of  $\text{Fe}^{2+}$ , higher ion diffusion rate, and lower electrode passivation during the process driven by PDC, which are further confirmed by electrochemical experiments driven by AL-TENG with a specific pulse signal. Additionally, with only the electrical energy extracted from water flow by the R-TENG, heavy

metal pollutant such as Cr(VI) can be sufficiently and continuously removed. Our findings not only establish optimization methodologies for electrochemical removing Cr (VI), but also provide a promising application of the self-powered system based on TENG for the simultaneous energy saving and environmental governance.

## 4. Experimental section

### 4.1. Fabrication of the AL-TENG

To serve as the substrate, kapton film with  $130 \mu\text{m}$  was folded into zigzag with 14 layers. Rectangle copper film with an area of  $5 \times 5 \text{ cm}^2$  was attached to both sides of Kapton film. Then fluorinated ethylene propylene (FEP) film with  $30 \mu\text{m}$  was stuck on same side of Cu layer in alternate structure.

### 4.2. Fabrication of R-TENG

**Rotor:** (1) As the triboelectric layer, acrylic with a thickness of  $5 \text{ mm}$  was cut to a disc-shaped with diameter of  $20 \text{ cm}$  by a laser cutter. The obtained acrylic arrayed radially with a central angle of  $3.75^\circ$  (2) For better installation, a through-hole was drilled at the center of the acrylic sheet. **Stator:** (1) To obtain a substrate, acrylic with a thickness of  $5 \text{ mm}$  was cut to a disc-shaped with diameter of  $20 \text{ cm}$  by a laser cutter. (2) Stick a prepared commercialized PCB on the substrate. Two sets of complementary radial-arrayed electrodes were designed on the PCB plate (a central angle of  $3.75^\circ$ ). (4) Due to electrical measurement or driven electrochemical reaction, the electrodes were connected to two lead wires, respectively. (5) A thin layer of kapton with  $30 \mu\text{m}$  was stuck onto the electrode layer.

### 4.3. Experiment of Cr(VI) removal

All the experiments for Cr(VI) treatment were carried out in a  $50 \text{ mL}$  electrolytic cell with  $30 \text{ mL}$  of potassium dichromate ( $\text{K}_2\text{Cr}_2\text{O}_7$ ) including different concentration of  $\text{NaCl}$  as electrolyte, where cylindrical graphite with diameter of  $0.6 \text{ cm}$  was acted as cathode and iron with an area of  $2 \text{ cm}^2$  was served as anode without adjusting pH. Before all the experiments, electrodes were washed with distilled water and then dried. During the process of the experiments, the applied electrodes were kept parallel at a distance of  $\sim 2.5 \text{ cm}$ . At set intervals, the concentration of Cr(VI) in the samples were gathered to detect. For Cr(VI) removal driven by TENGs, a rectifying bridge was used to convert the alternating current to direct pulse current signals. For self-powered system, the central of R-TENG (diameter of  $14 \text{ cm}$ ) and the fabricated water turbine were joined together. Normal water was injected into the water turbine to drive electrochemical reaction through R-TENG. All the experimental was conducted at ambient temperature.

### 4.4. Characterization

A linear motor was used to control the contact-separation process. A commercial motor was applied to drive the rotary process. The short circuit current and transferred charges of the TENG were measured using a programmable electrometer (keithley model 6514). The open circuit voltage of the TENG was tested by a Mixed Domain Oscilloscope (MDO3024). The chemical structures were measured through an X-ray photoelectron spectroscope (XPS, Thermo Escalab 250XI, USA). The Cr (VI) concentration was tested using an ultraviolet-visible (UV-vis) spectrophotometer (UV 2600) at the maximum absorption wavelength of  $540 \text{ nm}$  with diphenylsemicarbazide serving as an indicator. The total concentration of Cr and Fe ions were measured using an inductively coupled plasma-optical emission spectrometer (ICAP7200).

## Acknowledgements

Research was supported by the National Key R & D Project from Minister of Science and Technology (2016YFA0202704), Beijing Municipal Science and Technology Commission (Z171100000317001, Z171100002017017, Y3993113DF), National Natural Science Foundation of China (Grant No. 61774016, 51432005, 5151101243, 51561145021).

## Appendix A. Supplementary data

Supplementary data to this article can be found online at <https://doi.org/10.1016/j.nanoen.2019.103915>.

## References

- [1] M. Elimelech, W.A. Phillip, *Science* 333 (2011) 712–717.
- [2] L.L. Zhou, G.L. Zhang, M. Wang, D.F. Wang, D.Q. Cai, Z.Y. Wu, *Chem. Eng. J.* 334 (2018) 400–409.
- [3] A. Zhitkovich, *Chem. Res. Toxicol.* 24 (2011) 1617–1629.
- [4] X. Su, A. Kushima, C. Halliday, J. Zhou, J. Li, T.A. Hatton, *Nat. Commun.* 9 (2018) 9.
- [5] C.E. Barrera-Diaz, V. Lugo-Lugo, B. Bilyeu, *J. Hazard Mater.* 223 (2012) 1–12.
- [6] M. Kikuchi, A. Syudo, M. Hukumori, C. Naito, J. Sawai, *Chemosphere* 170 (2017) 113–117.
- [7] L.F. Zhang, W. Xia, X. Liu, W.Q. Zhang, *J. Mater. Chem. 3* (2015) 331–340.
- [8] S. Rengaraj, C.K. Joo, Y. Kim, J. Yi, *J. Hazard Mater.* 102 (2003) 257–275.
- [9] Y.L. Zhong, X. Qiu, D.Y. Chen, N.J. Li, Q.F. Xu, H. Li, J.H. He, J.M. Lu, *ACS Appl. Mater. Interfaces* 8 (2016) 28671–28677.
- [10] W. Jin, H. Du, S.L. Zheng, Y. Zhang, *Electrochim. Acta* 191 (2016) 1044–1055.
- [11] S. Elabbas, N. Ouazzani, L. Mandi, F. Berrekhis, M. Perdicakis, S. Pontvianne, M.N. Pons, F. Lapicque, J.P. Leclerc, *J. Hazard Mater.* 319 (2016) 69–77.
- [12] E. Keshmirizadeh, S. Yousefi, M.K. Rofouei, *J. Hazard Mater.* 190 (2011) 119–124.
- [13] Z.H. Yang, H.Y. Xu, G.M. Zeng, Y.L. Luo, X. Yang, J. Huang, L.K. Wang, P.P. Song, *Electrochim. Acta* 153 (2015) 149–158.
- [14] Y. Yang, H.L. Zhang, S. Lee, D. Kim, W. Hwang, Z.L. Wang, *Nano Lett.* (2013) 803–808.
- [15] Z.L. Li, J. Chen, J. Yang, Y.J. Su, X. Fan, Y. Wu, C.W. Yu, Z.L. Wang, *Energy Environ. Sci.* 8 (2015) 887–896.
- [16] M.H. Yeh, H. Guo, L. Lin, Z. Wen, Z. Li, C. Hu, Z.L. Wang, *Adv. Funct. Mater.* 26 (2016) 1054–1062.
- [17] Z. Li, J. Chen, H. Guo, X. Fan, Z. Wen, M.H. Yeh, C. Yu, X. Cao, Z.L. Wang, *Adv. Mater.* 28 (2016) 2983–2991.
- [18] Z. Li, J. Chen, J. Zhou, L. Zheng, Ken C. Pradel, X. Fan, H. Guo, Z. Wen, M.H. Yeh, C. Yu, Z.L. Wang, *Nano Energy* (22) (2016) 548–557.
- [19] J. Wang, C.S. Wu, Y.J. Dai, Z.H. Zhao, A. Wang, T.J. Zhang, Z.L. Wang, *Nat. Commun.* 8 (2017) 8.
- [20] W.L. Liu, Z. Wang, G. Wang, G.L. Liu, J. Chen, X.J. Pu, Y. Xi, X. Wang, H.Y. Guo, C.G. Hu, Z.L. Wang, *Nat. Commun.* 10 (2019) 9.
- [21] J. Wang, S.M. Li, F. Yi, Y.L. Zi, J. Lin, X.F. Wang, Y.L. Xu, Z.L. Wang, *Nat. Commun.* 7 (2016) 8.
- [22] M.H. Yeh, L. Lin, P.K. Yang, Z.L. Wang, *ACS Nano* 95 (2015) 4757–4765.
- [23] Q. Tang, M.H. Yeh, G. Liu, S. Li, J. Chen, Y. Bai, L. Feng, M. Lai, K.C. Ho, H. Guo, C. Hu, *Nano Energy* 47 (2018) 74–80.
- [24] M. Al-Shannag, Z. Al-Qodah, K. Bani-Melhem, M.R. Qtaishat, M. Alkasrawi, *Chem. Eng. J.* 260 (2015) 749–756.
- [25] E. Gatsios, J.N. Hahladakis, E. Gidarakos, *J. Environ. Manag.* 154 (2015) 117–127.
- [26] I. Linares-Hernandez, C. Barrera-Diaz, G. Roa-Morales, B. Bilyeu, F. Urena-nunez, *Chem. Eng. J.* 148 (2009) 97–105.
- [27] Y.S. Tian, W.H. He, X.P. Zhu, W.L. Yang, N.Q. Ren, B.E. Logan, *Chem. Eng. J.* 292 (2016) 308–314.
- [28] M.G. Arroyo, V. Perez-Herranz, M.T. Montanes, J. Garcia-Anton, J.L. Guinon, *J. Hazard Mater.* 169 (2009) 1127–1133.
- [29] P.N. Johnson, A. Amirtharajah, *J. Am. Water Work. Assoc.* 75 (1983) 232–239.
- [30] M.Y.A. Mollah, R. Schennach, J.R. Parga, D.L. Cocke, *J. Hazard Mater.* 84 (2001) 29–41.
- [31] J.C. Shu, R.L. Liu, Z.H. Liu, J. Du, C.Y. Tao, *Sep. Purif. Technol.* 168 (2016) 107–113.
- [32] A.K. Golder, A.N. Samanta, S. Ray, *J. Hazard Mater.* 141 (2007) 653–661.
- [33] B.M. Sass, D. Rai, *Inorg. Chem.* 26 (1987) 2228–2232.
- [34] L.L. Zhou, R.R. Li, G.L. Zhang, D.F. Wang, D.Q. Cai, Z.Y. Wu, *Chem. Eng. J.* 339 (2018) 85–96.
- [35] Y.L. Zhang, Y.M. Li, J.F. Li, G.D. Sheng, Y. Zhang, X.M. Zheng, *Chem. Eng. J.* 185 (2012) 243–249.
- [36] X. Yin, D. Liu, L.L. Zhou, X.Y. Li, C.L. Zhang, P. Cheng, H.Y. Guo, W.X. Song, J. Wang, Z.L. Wang, *ACS Nano* 13 (2019) 698–705.